AAS 11-182

LOW ALTITUDE MAPPING ORBIT DESIGN AND MAINTENANCE FOR THE DAWN DISCOVERY MISSION AT VESTA

Gregory J. Whiffen*

NASA's Dawn discovery mission will orbit the giant asteroid Vesta beginning in the summer of 2011. Four different near polar science orbits are planned. The lowest planned orbit at Vesta is called the Low Altitude Mapping Orbit or LAMO and is by far the most challenging to design and maintain due to the strong, non-spherical gravity expected there. This paper describes the orbit selection process. The true gravity field of Vesta remains highly uncertain. The proposed orbit selection process will be applied once sufficient gravity knowledge is obtained at higher orbits. The orbit selection process is applied here to a fictitious gravity field based on a Hubble space telescope shape model for Vesta assuming uniform density. The outcome of the process described here is a variety of stable orbits. However, Initially stable orbits at the LAMO altitude are not expected to remain stable operationally due to the unpredictable impulses resulting from the Dawn spacecraft thruster firings to de-saturate its momentum wheels. As a result, orbital maintenance maneuvers will be probably be necessary. This paper also briefly describes the statistical maneuver design process that resulted in the orbit maintenance plan.

INTRODUCTION

The science objectives of the NASA Dawn Discovery mission are to explore the largest two members of the main asteroid belt.[1] Both Vesta and Ceres are proto planets that failed to grow to a much larger size as a result of the gravitational disruption caused by the rapid formation of Jupiter. NASA's Dawn discovery mission will enter orbit around the giant asteroid Vesta in the summer of 2011. Four different near polar science orbits are planned. The lowest planned science orbit at Vesta is called the Low Altitude Mapping Orbit or LAMO. This science orbit averages about 460 [km] radius and is by far the most challenging to design and maintain due to the strong, non-spherical gravity expected there. The Dawn spacecraft uses solar electric propulsion for all transfer maneuvers and orbit maintenance maneuvers. This paper describes the orbit selection process that will be used at Vesta. The true gravity field of Vesta remains highly uncertain. The proposed orbit selection process will be applied once sufficient gravity knowledge is obtained at earlier, higher orbits. In order to illustrate the proposed orbit selection process, it is applied here to a fictitious field based on a Hubble space telescope shape model[2] for Vesta assuming a uniform density. The uniform density gravity model used in this analysis was developed by Alex Konopliv of the Jet Propulsion laboratory. Vesta is a differentiated body so the assumption of uniformity is not likely. Vesta suffered an enormous impact that removed and altered material on a global scale. As a result little can be known about Vesta's internal structure and therefore the uniform density model is as good an approximation as any other currently available. Given Vesta's complex shape and large size, the uniform density model generates a challenging gravity field for this analysis.

* Senior Engineer, Mission Design and Navigation Section, Jet Propulsion Laboratory, 4800 Oak Grove Drive, Pasadena, California 91109

In this paper, Stable orbits mean orbits that have stable orbital planes (ideally Sun synchronous). Orbits that impact the surface of Vesta as a result of instability do not appear to be a threat at the LAMO altitude given the shape of Vesta. However, any orbit that has a rapidly changing plane can place the spacecraft in danger and must be avoided. The Dawn spacecraft has an operational constraint that requires that it is never thermally cycled by repeatedly entering and exiting shadow. For this reason, orbits with stable, Sun synchronous planes must be found and targeted. Orbits that have an initially stable orbit plane but easily develop a rapidly changing orbit plane due to small perturbations must be avoided. An additional constraint on any orbit maintenance plan is the spacecraft must be able to avoid shadow even when there is a loss of control for four weeks (for example missing all orbital maintenance maneuvers during this time). This constraint is necessary so severe spacecraft safing events can be tolerated.

Candidate Low Altitude Mapping Orbits (LAMOs) must be screened for ground track coverage in addition to orbit stability characteristics. The ground track requirement is easily met by any orbit that maintains a stable plane and has any of a wide range of mean geometric periods. A method and classification system has been developed to identify satisfactory orbits. The approach described here relies on a grid search in a 4 dimensional state space. The approach is computationally expensive, but is suited to parallel processing.

APPROACH

The goal of this analysis is to find initial conditions for orbits that are inherently stable, and exhibit a zero or slow, constant rate of plane change moving away from Vesta shadow. The grouping of candidate orbits is best done by measuring their mean geometric orbital periods. At LAMO altitudes, oscillating periods oscillate wildly and are not useful for measurement. Hence the need for considering geometric periods. However, even geometric period will vary in a repeating pattern so the most useful measure is the mean geometric period averaged of many orbits. The radius of LAMO is expected to be near 460 kilometers but maybe 10s of kilometers lower or higher depending on the orbits that exist in the gravity that will be discovered. Science requirements can be met at this altitude given enough time. Lower altitudes are desirable but cost science time by requiring longer (and riskier) transfers to reach them.

The method used to perform a comprehensive exploration of the design space is based on a four dimensional grid search. There are seven dimensions available to a general orbit around a non-spherical body that is undergoing a simple rotation. Six degrees of freedom correspond to initial position and velocity of the spacecraft and the seventh is the epoch of the initial condition. The epoch of the initial condition determines the orientation of the central body. The Low Altitude Mapping Orbit is required to be near circular and its orbit plane must be oriented so that its orbit plane is 45 degrees away from the Sun direction to satisfy science objectives. A further constraint is that the orbit descending node must be over the lit AM side of Vesta. These requirements fully determine the orbit plane. In a point mass two-body system, constraining the orbit plane removes two degrees of freedom and constraining the eccentricity removes a third degree of freedom and also a fourth if the eccentricity happens to be zero (argument of periapsis then becomes irrelevant). So for the LAMO design space, constraining plane and eccentricity to near zero leaves seven minus four or only three degrees of freedom. However, the (mean) eccentricity of LAMO is not (and cannot be) strictly constrained to be zero. The mean eccentricity does not need to fully minimized to achieve science objectives, so there is a bounded degree of freedom that remains. This leaves four degrees. The orbit size is bounded by the maximum range that is acceptable to science and the

minimum range that is both safe and practical to reach.

There are many possible parameterizations of the remaining four degrees of freedom. The simplest to implement is a set of oscillating orbital elements at a fixed epoch. The set chosen here are semi-major axis, eccentricity, argument of the periapsis, and inclination. The meaning of each of these elements is blurred when viewed in terms of the corresponding orbit properties or mean elements. However the following interpretations are postulated. The semi-major axis mainly controls the orbital energy (Vesta rotational phase also controls the initial orbital energy). Eccentricity mainly control orbit shape, searching the phase space of orbits that start in a direction that is above and below the local horizontal direction. The argument of periapsis (given a fixed true anomaly) effectively controls the Vesta rotational phase because it determines where around Vesta the orbit starts given a non-zero eccentricity. Inclination mainly controls the orbit plane change rate as a result of nodal precession primarily due to J2. All four elements impact mean geometric period and the nodal precession as a result of the J2 and the strong higher order gravity terms. Taken as a whole, all four elements adequately (though not precisely) cover the desired 4 degrees of freedom remaining in the orbit design phase space. The objective of a grid search over the four dimensions defined above is to search for useful specific orbit, useful patterns, and determine what LAMO properties are possible in general.

The grid sample space is defined in Table 1 corresponding to a total of 276 x 6 x 12 x 5 = 99,360 points. Each point results in an initial condition that can be propagated to measure orbit plane evolution and mean geometric period. The ranges and step sizes chosen in Table 1 were selected based judgment made from many individual test propagations. The results from this set of points appears to yield a near exhaustive search. Note that propagation of these initial states alone does not determine the stability of the corresponding orbits they define. Another step is necessary. This step will be presented later.

Table 1. LAMO grid sample points

Semi-major Axis	425 to 480 [km] in 200 [m] steps
Eccentricity	0, 0.005, 0.010, 0.015, 0.020 0.025
Argument of the Periapsis	0, 30, 60, 90, 120, 150, 180,210, 240, 270, 300, 330 [degrees]
Inclination	90, 90.10, 90.15, 90.20, 90.25

RESULTS OF THE GRID SEARCH

Nonlinear propagation of the grid point initial states assumed an 8x8 harmonic approximation of the the uniform density Vesta model. The 40 day propagations result in about 240 orbital revolutions. About 2000 propagations per day per cpu are possible. Since each propagation is independent of the next, it is easy to deploy this process to a large computer cluster. Figure 1 presents a histogram of the resulting orbital mean geometric periods for all of the grid point initial conditions. The range of mean geometric periods obtained from the grid search is from 3.5 to 4.8 [hours] which completely brackets the desired LAMO period of 4.1 hours. Despite an even grid spacing and a very large sample space, the mean geometric period remains highly clumped. Figure 1 indicates various Vesta rotational to spacecraft orbital resonances with labeled red, vertical lines. In some cases, resonances appear to “repel” trajectories. Sometimes the repulsion is symmetric and sometimes it is asymmetric about the resonance. Clumping appears above several of the strong (low order)

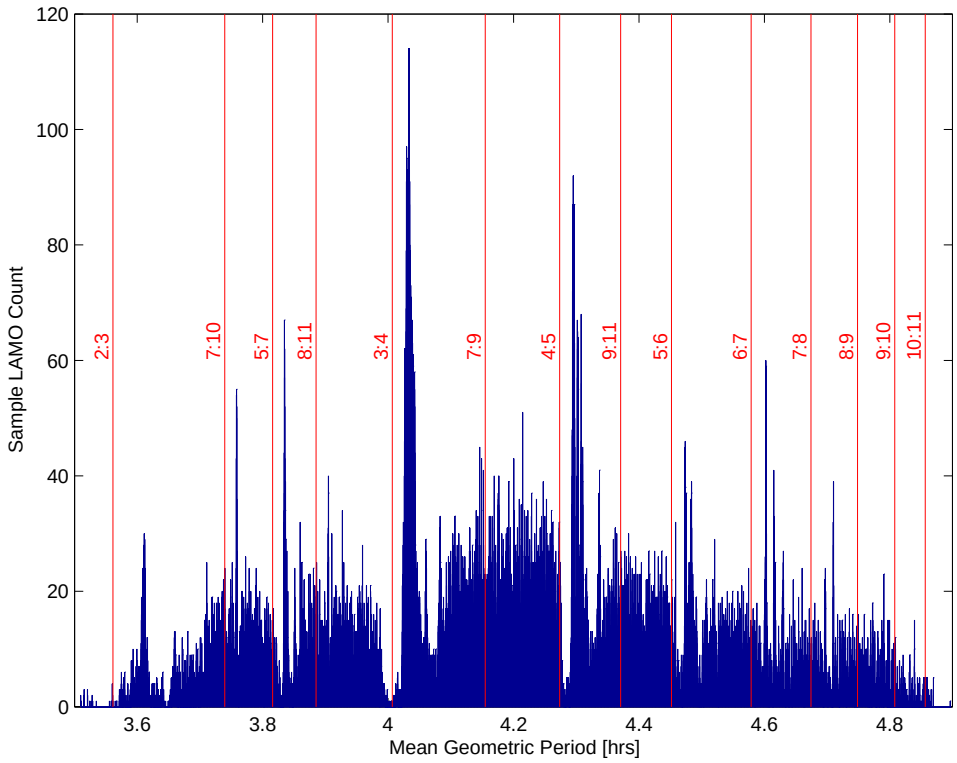

Figure 1. A histogram of the mean geometric periods of all orbits in the search. Vesta rotational to spacecraft orbital resonances are indicated by red vertical lines. The mean geometric periods are highly clumped.

resonances like the 3:4, 4:5, and 5:6 resonances. This may indicate inherent stability above certain resonances. The most repellant resonance is 3:4. The repulsion is symmetric. This may indicate that very few stable orbits exist with mean geometric periods very close to the 3:4 resonance. Another observation that can be made is that there are smaller clumps and repulsive periods not associated with any low order resonance. Part of this may be due to the fact that there may be orbits which transition from one pseudo stable geometric period to another (and possibly back again). If this is the case, then this may obscure the repelling/attracting periods in the mean period plot in Figure 1. To investigate this possibility, Figures similar to 2 were generated. Figure 2 is a plot of geometric period (not **mean** geometric period) versus propagation time for all 99,360 grid search orbits. In this Figure, geometric period is computed as a running value based on the immediately previous full revolution. Color in Figure 2 is determined by the **mean** geometric period. There is both a long term and short term oscillation in the geometric period for all orbits. The short term oscillation period is a function of the mean geometric period. The short term oscillation has a period of about 24 hours near a mean geometric period of 4.9 hours and decreases to 10.5 hours at a mean geometric period of 3.5 hours. The long term oscillation in geometric period appears to not be a strong function of geometric period. For the range of mean geometric periods considered (3.5 to 4.9 hours) the long term oscillation period is near 9.0 days. These characteristics are of interest to the science planning for the Low Altitude Mapping Orbit, but will likely change quantitatively once the true Vesta gravity field is determined. Clumping is much less clear when orbit to orbit variation in geometric period is plotted as in Figure 2. It is also interesting that there is a great deal of apparent instability near

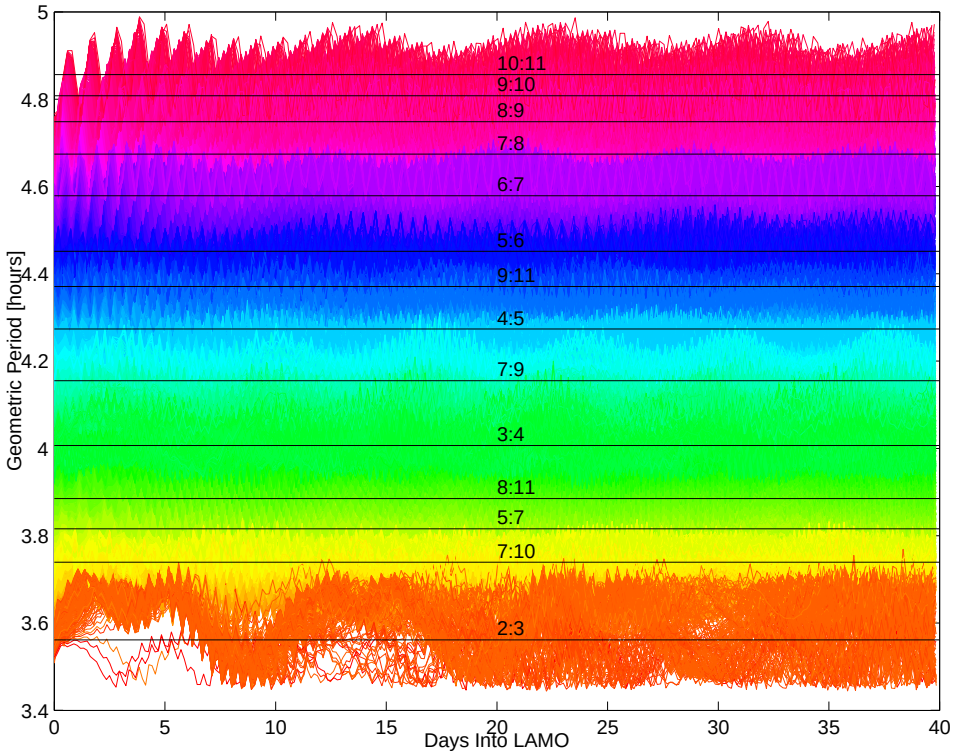

Figure 2. Geometric period (not mean geometric period) versus propagation time for all grid point orbits. Color in Figure 2 is determined by the mean geometric period.

the 2:3 resonance at the bottom of Figure 2. The red and orange colors indicating different mean geometric periods are often on top of each other in this plot which indicates that transitions from one pseudo stable geometric period to another and back again does occur for some orbits.

An important characteristic for the selection of an acceptable orbit is the mean radius. The mean radius controls the resolution of Dawn's Gamma Ray and Neutron Detector (GRAND) instrument[1] and the resolution of imaging instruments. GRAND is one of two primary experiments for LAMO. The other is gravity science which is also strongly influenced by mean radius. Figure 3 is a plot of all grid orbit's mean geometric period versus mean radius. Color is scaled to mean geometric period. Mean radius is computed by averaging over the full 40 day propagation (or over approximately 240 revolutions). A significant feature of Figure 3 is that there is not a one to one correspondence between mean radius and mean geometric period. Specifically, for a given mean geometric period, orbits with different mean radii generally (but not always) exist. Similarly, for a given mean radius, multiple orbits may exist with different mean geometric periods. Figure 4 is a small part of the data presented in Figure 3 which emphasizes that multiple orbits at given mean radii or mean geometric period exist. Figure 4 also indicates that there are complex patterns present in the fine structure of the mean geometric period versus mean radius relationship.

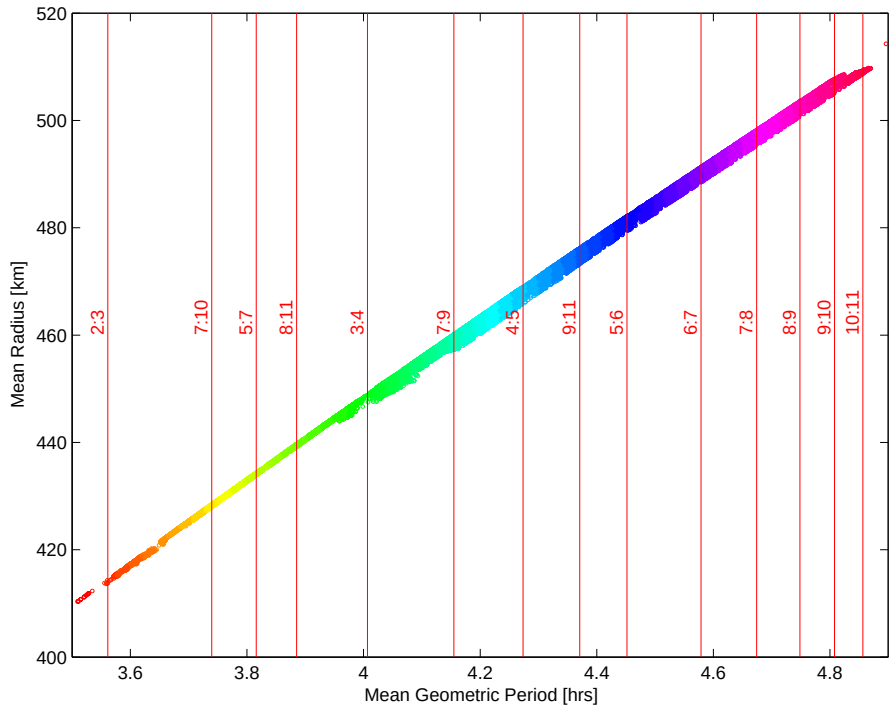

Figure 3. Mean geometric period versus mean orbital radius for all grid point orbits. Color in determined by the mean geometric period.

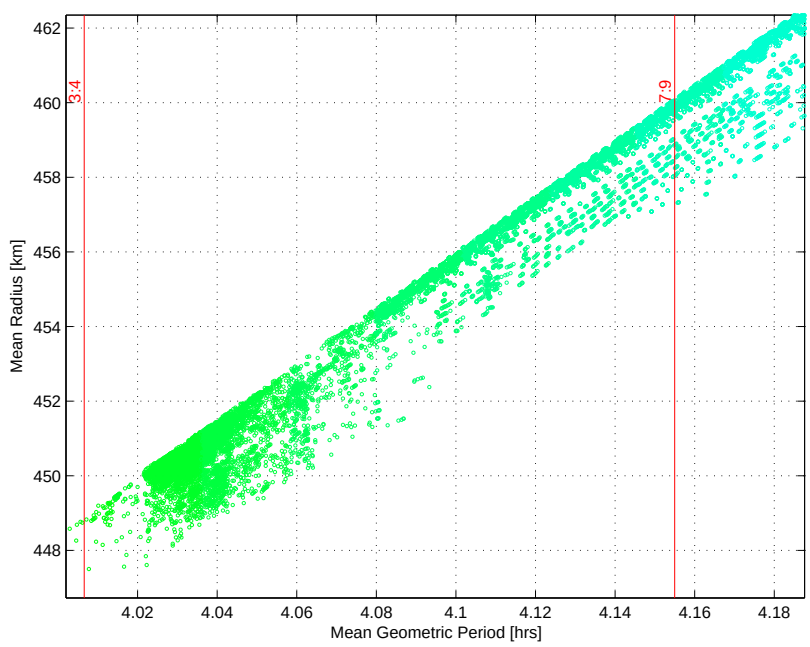

Figure 4. Mean geometric period versus mean orbital radius for a subset of orbits.

Another important characteristic for the selection of an acceptable orbit is the Sun "β" angle. The Sun β angle is the angle between the orbit plane (not the angular momentum unit vector) and the Sun direction. A β angle of 90 degrees corresponds to an orbit that is face on to the Sun. A β angle of 0 degrees corresponds to an orbit that is edge on to the Sun. Angles lower than about 39 degrees will place Dawn in repeated shadow from Vesta when near the LAMO altitude. The Dawn spacecraft has an operational constraint that it must not enter shadow to avoid thermal cycling. The minimum safe β angle that can be targeted has been established to be 45 degrees. Figure 5 presents the time evolution of the β angle for all orbits. Again, colors indicate different mean geometric periods. Notice that all orbits in Figure 5 begin near the minimum safe target of 45 degrees β angle.

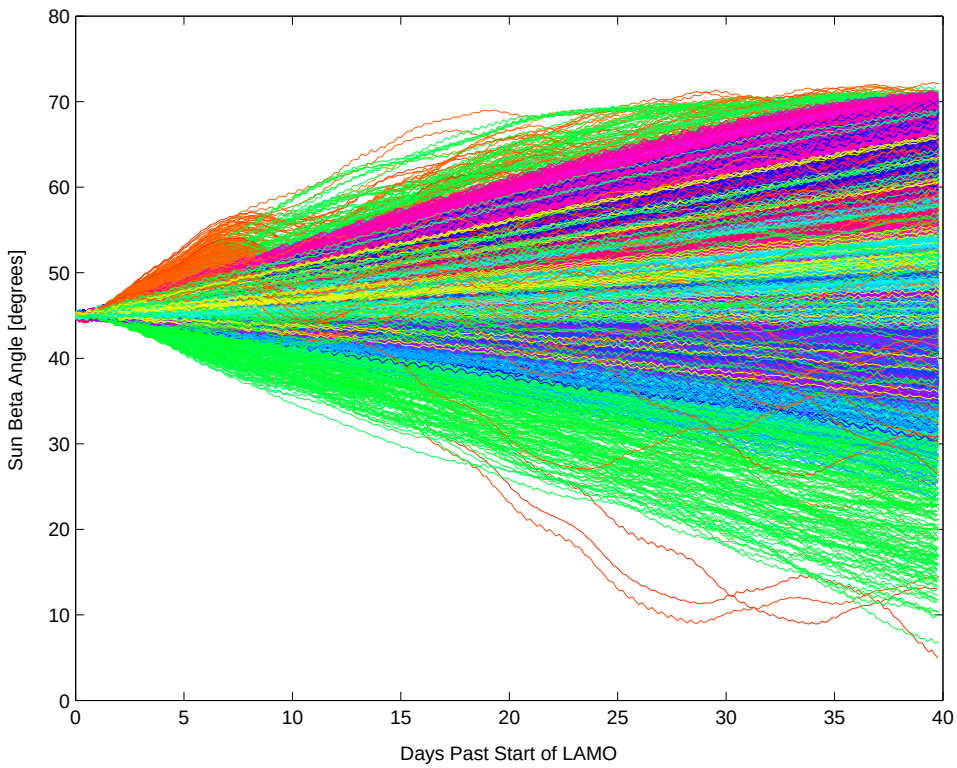

Figure 5. The time evolution of the β angle for all orbits. Note that all orbits begin near the desired value of 45 degrees. Orbits that move below 39 degrees enter Vesta shadow.

However, a great many orbits have a downward trend. It should be noted that the maximum β angle possible in LAMO orbit is a little above 70 degrees as a result of the particular pole of Vesta and the requirement that LAMO is near polar. Therefore in Figure 5 orbits with rapidly increasing β angles appear to "bounce" off of a β angle of 70 degrees and then head downward. The rate of change of the orbit plane in all cases changes roughly linearly over time scales of 10 days or more.

SCREENING THE GRID SEARCH RESULTS

One desired characteristic of LAMO is a near flat time evolution of the β angle. The reasons for this are (1) we stay near the minimum safe β angle for optimal lighting for imaging and (2) we end LAMO with a low enough β angle to be able to reach the next science orbit HAMO2 which is desired to have a β angle of 45 degrees also. If we depart LAMO with a β angle much larger

than 45 degrees then the large cost of the plane change will delay the start of and reduce the size of HAMO 2. Using the instability of the 1:1 resonance on the way to HAMO 2 to achieve a "free" plane change is considered too risky because any useful orbit will have to have a rapid naturally declining β angle. Any temporary loss of spacecraft control will result in the spacecraft staying in the declining β angle trajectory too long which will result in shadow entry.

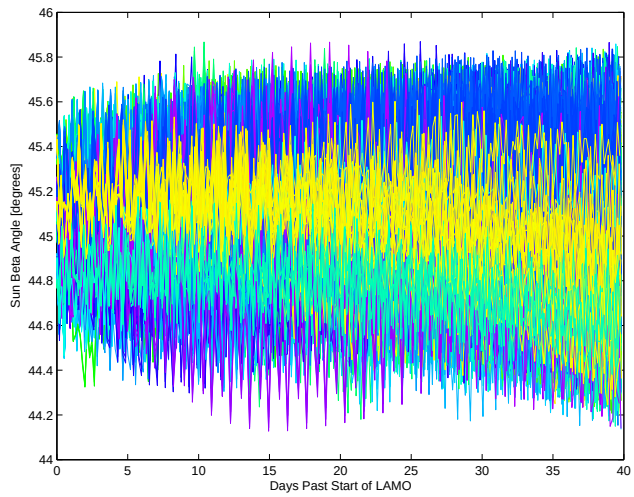

Figure 6. The time evolution of the β angle for all orbits that stay between 44 and 46 degrees β angle. Different colors indicate different mean geometric periods.

A total of 992 distinct orbits remain if all orbits with β angle rates that cause them to depart the β angle range of 44 to 46 degrees during the 40 day propagation are removed. The β angle evolution of the remaining 992 orbits are plotted in Figure 6. Slowly evolving β angle orbits exist at a wide range of mean geometric periods. Figure 7 provides a histogram of the orbit mean geometric

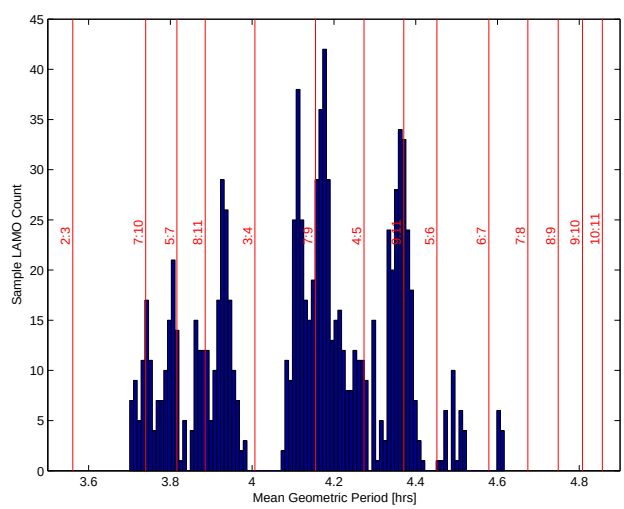

Figure 7. The time evolution of the β angle for all orbits that stay between 44 and 46 degrees β angle. Different colors indicate different mean geometric periods.

periods that satisfy the 44 to 46 degree β angle range. Notice that there are no orbits near the 3:4 resonance. Clearly this is a region to avoid. The largest concentration of orbits occur just above the 7:9 resonance at a mean geometric period of about 4.2 hours. This period corresponds to orbits with a mean radius of around 460 kilometers.

SCREENING FOR ORBIT STABILITY

Stability in this context refers only to the β angle rate. Orbits that impact the surface of Vesta as a result of instability do not appear to be a threat at the LAMO altitude given the shape of Vesta. Our delivery to the start of a selected LAMO will be imperfect. It is necessary to not only select an orbit with a very low β angle evolution rate but also one that is as stable as possible. Stability is not only required to account for a poor initial delivery to LAMO but also to absorb the unpredictable impulses resulting from the Dawn spacecraft thruster firings to de-saturate its momentum wheels. These thruster firings are not generally symmetric so there are usually small net impulses associated with them.

Orbit stability is tested through introducing carefully selected phase space perturbations at the start of an orbit and tracking the divergence of the β angle compared to the unperturbed trajectory. The first step is to estimate a "typical" distribution of expected LAMO initial delivery errors in position and velocity (phase) space. To obtain this distribution, a Monte Carlo simulation of nonlinear propagations and non-linear optimization subject to sampled orbit determination error, gravity knowledge error, momentum de-saturation uncertainty, and transfer maneuver execution error was used to model the transfer leading up to LAMO.[3] The resulting Monte Carlo deliveries to LAMO are fit with a phase space (6 x 6) covariance matrix. The method described here is not very sensitive to the assumed distribution of expected trajectory perturbations. The main purpose of the distribution is to provide an approximate shape of typical dispersions in phase space. For example, down-track perturbations are typically much larger than cross track perturbations for orbital missions. A covariance matrix model developed in the way described above will exhibit this shape.

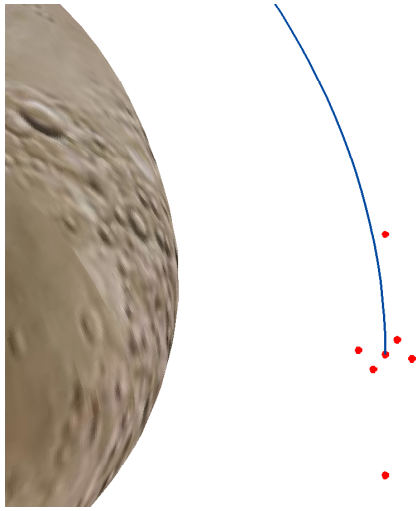

Figure 8. An example of 6 position displacements developed from eigen vectors. The position displacements are centered on a blue reference trajectory. The size of the displacements are exaggerated for illustrative purposes.

The second step is to compute six independent Eigen vectors of the covariance and also record

the reverse directions of these six Eigen vectors. The result is twelve displacements in the six dimensional position-velocity phase space corresponding to a single standard deviation perturbation. Using these twelve displacements rather than randomly sampling the covariance greatly reduces the required number of displacements need to characterize the phase space encompassing typical LAMO start delivery errors. This approach is similar to the previously developed sigma point methods for Kalman filters[4] and unscented filtering methods for nonlinear estimation.[5] Figure 8 is an example of 6 position space displacements about the reference propagation (blue trajectory). This approach is also used to evaluate the stability of the powered flight periods during transfers at Vesta.[6] The covariance used in this analysis was developed using a Monte Carlo process[3] and is provided in Table 2. The covariance is provided in the Radial, Transverse, and Normal (RTN) frame. The most useful frame in which to compute the covariance and resulting eigen vectors is in the RTN frame. The RTN frame is defined as follows. The radial direction is defined as the (outward) directed direction from the central body to the spacecraft, the transverse direction is defined as the local horizontal direction closest to the orbital velocity, and the normal direction completes the right handed, orthonormal coordinate system. The advantage of using this frame is that the resulting twelve displacements in phase space can be applied at any point around an orbit. The upper left 3 x 3 position sub-matrix norm of the covariance in Table 2 is 1.9865 [km]. The lower right 3 x 3 velocity sub-matrix norm of the covariance in Table 1 is 0.7785 [m/s].

Table 2. LAMO initial delivery characteristic covariance in the RTN frame [km,s]

0.027798	-0.32469	-0.001504	0.00012762	-4.5042e-6	5.7168e-7
-0.32469	3.9191	0.016945	-0.0015402	5.3174e-5	-7.2113e-6
-0.001504	0.016945	0.00082985	-6.6637e-6	2.1481e-7	-3.3367e-8
0.00012762	-0.0015402	-6.6637e-6	6.0533e-7	-2.0907e-8	2.8349e-9
4.5042e-6	5.3174e-5	2.1481e-7	-2.0907e-8	7.8476e-10	-9.19e-11
5.7168e-7	-7.2113e-6	-3.3367e-8	2.8349e-9	-9.19e-11	2.5959e-11

The first six cloud states are derived from the covariance in Table 2 as follows

$$\Delta State_i = COV_{cholesky} \cdot EV_i \cdot s \qquad for\ i = 1, 2, 3, 4, 5, 6 \tag{1}$$

where $COV_{cholesky}$ is the lower triangular Cholesky factor of the covariance, EV_i is the ith eigen vector of the covariance, and s is the "sample depth" (or sigma depth). In this analysis, $s = 2$ meaning the state cloud is of size two standard deviations according to the covariance used. The remaining 6 cloud states are

$$\Delta State_i = -\Delta State_{i-6} \qquad for\ i = 7, 8, 9, 10, 11, 12. \tag{2}$$

The third and final step is to use the set of twelve displacements in phase space to create state clouds around the initial condition of each orbit to be tested. Each state is propagated forward in time using fully nonlinear propagation while recording the β angle evolution of each state. Relatively rapid divergence of one or more cloud states β angle indicates instability. A criteria for "stable enough" depends on the orbit maintenance plan (covered later) and the ability to survive a temporary loss of spacecraft control without entering shadow.

The method outlined above was applied to the boxed portion of the screened trajectories illustrated in Figure 9. Figure 9 includes only orbits that stay within a β angle range of 44 to 46 degrees.

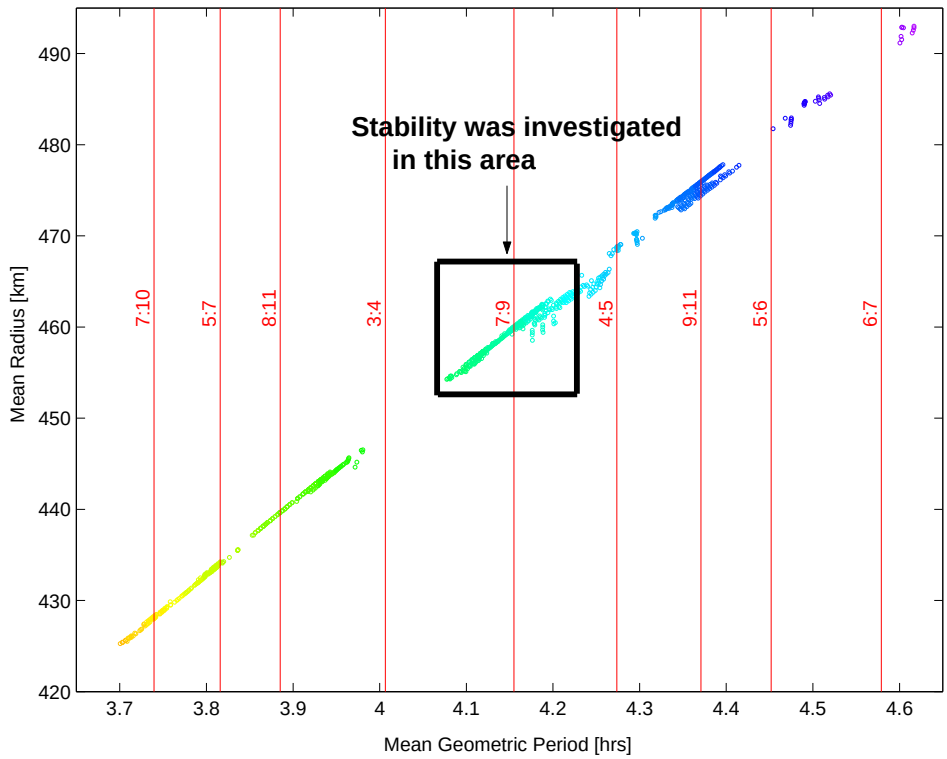

Figure 9. Mean geometric period versus mean orbital radius for orbits that stay within a β angle range of 44 to 46 degrees. Color in Figure is determined by the mean geometric period.

Of these orbits it was determined for a variety of reasons to focus on orbits between the 3:4 and 4:5 resonance. Figure 10 illustrates the subset of orbits inside the box in Figure 9. The stability analysis described above was applied to the orbits labeled 12 through 21 in Figure 10. Based on the results of an analysis of a large number of orbits, a stability classification system was developed based on the maximum excursion of the β angle over all twelve perturbed orbits relative to the nominal unperturbed orbit given 1 40 day or 240 orbital revolutions. A 2σ perturbation cloud is assumed in the classification system. Table 3 presents the classification system. Stability in this classification system is purely relative based on the range of stability found in the entire grid search. The approx-

Table 3. LAMO orbit relative stability classification system

Class	maximum β angle excursion during a 40 day propagation	Relative abundance
Ultra Stable	0° to 0.25^o Degrees	5%
Very Stable	0.25^o to 0.75^o Degrees	32%
Stable	0.75^o to 1.25^o Degrees	35%
Less Stable	1.25^o to 1.75^o Degrees	12%
Unstable	1.75^o to 2.50^o Degrees	10%
Very Unstable	$> 2.50^o$ Degrees	6%

imate relative abundances of the different levels of stability found in the grid search are included in

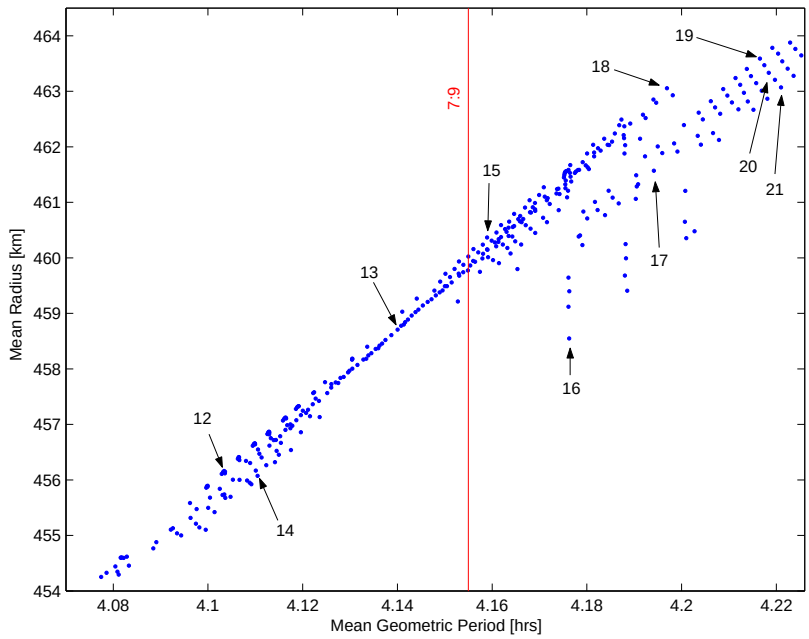

Figure 10. Mean geometric period versus mean orbital radius for orbits that stay within a β angle range of 44 to 46 degrees and have a mean geometric period that is near the 7:9 resonance. The results of a stability analysis will be presented for the orbits labeled 12 through 21.

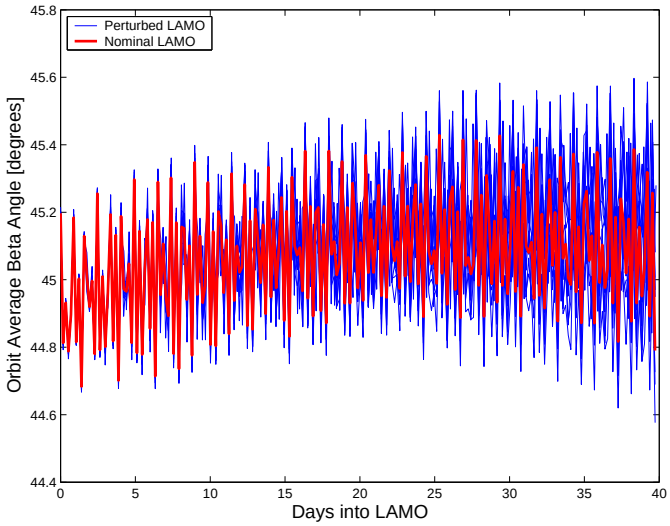

Figure 11. An example of an "ultra stable" orbit's time evolution of the β angle. The unperturbed orbit is plotted as a red line and each of the 12 two-sigma perturbed orbits are plotted with blue lines.

Table 3. An example of an "ultra stable" orbit is provided in Figure 11. Figure 11 corresponds to the orbit labeled 20 in Figure 10. The unperturbed orbit's time evolution of the β angle is plotted as a red line in Figure 11. Each of the 12 perturbed orbits are plotted with blue lines. There is very

little change in the β angle evolution given the 2σ perturbations. In fact this orbit can withstand 4σ perturbations and still stay below 0.5^o excursions from the unperturbed trajectory during a 40 day propagation. Orbits with this degree of stability are highly desirable. The fact that these orbits exist for the uniform density model of Vesta is no guarantee they will exist for the real Vesta gravity field that we will encounter. Another interesting feature of Figure 11 is the slight curvature of the time evolution of the β angle. This may be a very long period oscillation. This very gentle curvature is not of any practical concern because it turns out that the Dawn spacecraft thruster firings to desaturate its momentum wheels are strong enough to move us off of an ultra-stable orbit well before 40 days. Orbital maintenance maneuvers are necessary well before 40 days into LAMO to compensate. Figures 12 and 13 are examples of a "Stable" and a "Very Unstable" orbit corresponding to the orbits labeled 15 and 16 respectively in Figure 10. Figure 14 is the same as Figure 10 except

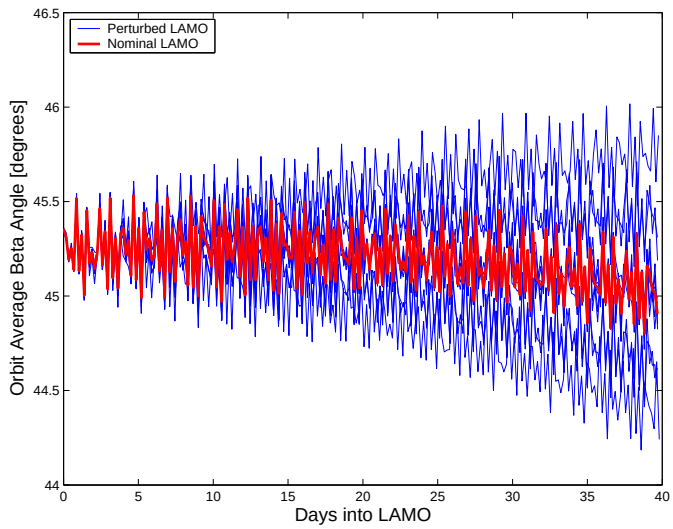

Figure 12. An example of a "stable" orbit's time evolution of the β angle. The unperturbed orbit is plotted as a red line and each of the 12 two-sigma perturbed orbits are plotted with blue lines.

the orbits labeled in Figure 10 have there stability indicated. It is interesting to see that the very regular pattern of orbits that exist in the upper right hand corner in Figures 10 and 14 are "ultra" stable. In general there is a great deal of interesting structure that can be seen in plots like Figure 14. The "thinning" of orbits that exist near orbit 13 in Figure 10 is also interesting. Near orbit 13 there appears to be only one mean radius orbit that exists for a given mean geometric period.

The "very unstable" orbit in Figure 13 demonstrates that, in some cases, only one of the twelve perturbations can diverge significantly. This is interesting because the opposite perturbation direction corresponding to this eigen vector is much more stable. Linear analysis would not predict this.

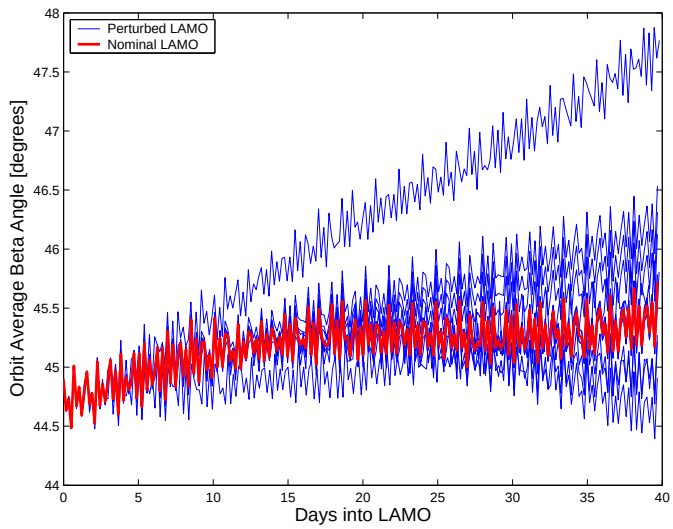

Figure 13. An example of a "very unstable" orbit's time evolution of the β angle. The unperturbed orbit is plotted as a red line and each of the 12 two-sigma perturbed orbits are plotted with blue lines.

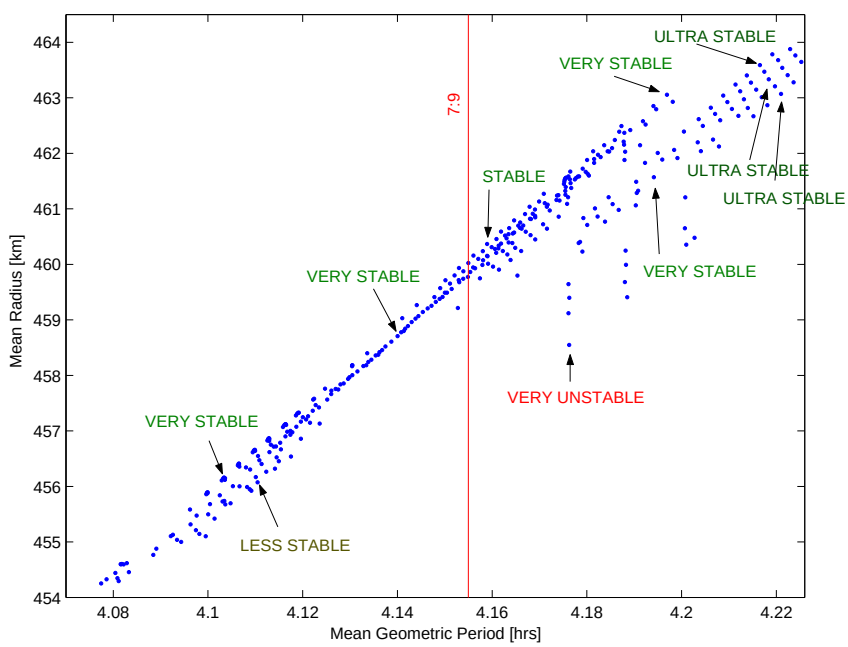

Figure 14. Mean geometric period versus mean orbital radius for orbits that stay within a β angle range of 44 to 46 degrees and have a mean geometric period that is near the 7:9 resonance. The results of a stability analysis for selected orbits are indicated.

LAMO ORBIT MAINTENANCE

Monte Carlo simulations indicate that even "ultra" stable orbits at LAMO altitudes, do not remain stable given the uncertainty of small velocity changes imparted from the asymmetric burns required for the Dawn spacecraft momentum wheel de-saturation. Therefore, it is necessary to develop an orbit maintenance plan. The fact that Dawn is an electric propelled spacecraft complicates the maneuver design. Further, given the dangerous operating conditions for the Dawn spacecraft at LAMO altitudes, the maintenance plan has to be robust against missed maintenance maneuvers. Specifically, temporary loss of control must not result in the spacecraft entering shadow. A fully nonlinear analysis is necessary to design and test any statistical maneuver plan and show that it is robust against missed maneuvers. Nonlinear analysis cannot be avoided due to the complex, nonlinear dynamics near Vesta. Candidate maintenance maneuver plans were evaluated by combining nonlinear propagation and optimization in a Monte Carlo loop with numerous error sources using Veil software developed by the author.[3] Error sources modeled include orbit determination error, maneuver execution error, missed maneuvers, gravity harmonics uncertainty, pole uncertainty, Vesta rotation uncertainty, momentum de-saturation burn uncertainty, and initial LAMO orbit injection errors. Each Monte Carlo run includes several orbit maintenance cycles daisy chained together to ensure instabilities in the control strategy do not emerge after repeated applications. The LAMO orbit is expected to last at least 70 days and possibly as long as 120 days. During this time Dawn will complete between 400 and 700 revolutions around Vesta. It was demonstrated that orbital maintenance maneuvers will be required on a weekly basis. Further, it was demonstrated that two maneuvers separated in time need to be designed simultaneously to correct orbit plane errors and regain orbital stability while remaining robust to missed maneuvers. The reasoning behind this architecture is presented in Figure 15.

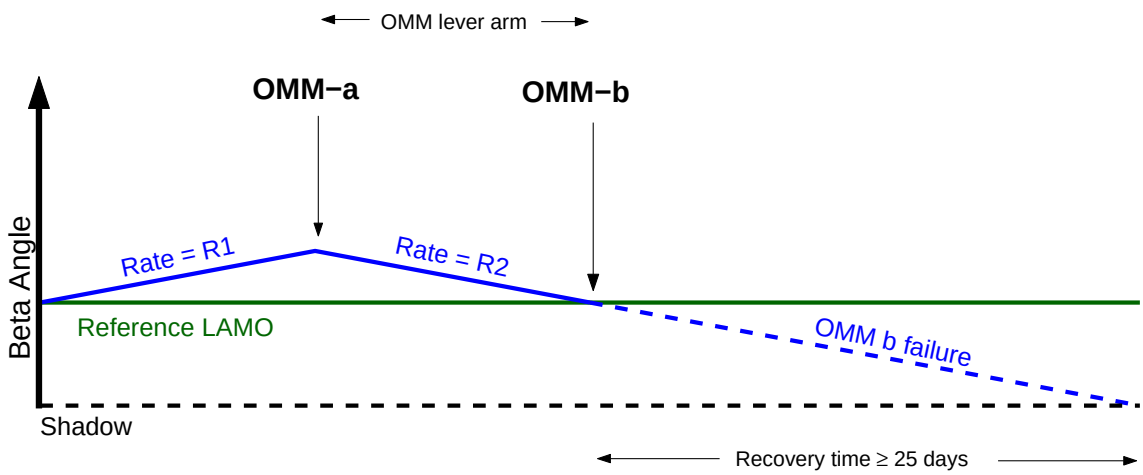

Figure 15. An example of correcting a LAMO that has a positive β angle rate using two simultaneously designed maneuvers OMM-a and OMM-b.

In general, a plane change (β angle change) and plane rate change cannot be corrected using a single low-thrust maneuver of acceptably short duration. Two maneuvers are therefore required. The first maneuver, "OMM-a" reverses the β angle rate so that after a period of time the β angle will return to the nominal value of 45°. When the orbit has returned to β=45° a second maneuver, "OMM-b", must then halt the β angle rate and retarget a stable (orbit plane) orbit. Figure 15 is an

example of correcting a LAMO that has a positive β angle rate. Its important to note that whenever a maneuver (OMM-a) is executed to create a negative β angle rate, and a second maneuver (OMM-b) to zero out the β angle rate is missed then shadow entry will occur after a certain period of time. The mission has a safety constraint that requires that shadow must always be avoided if control is lost for up 25 days. Therefore the negative β angle rate ($R2$ in Figure 15) must be gradual enough that shadow will be avoided for at least 25 days in the event of the OMM-b failure. This also means that the time between OMM-a and OMM-b must be long enough to accommodate the gradual rate set up by OMM-a (see Figure 15). The time between OMM-a and OMM-b is called the OMM lever arm time. The longer the lever arm, the more gradual the recovery rate $R2$ in Figure 15 can be. The maximum rate $R1$ in Figure 15 that we are likely to encounter (which is not in our control) and the reaction time or the time when OMM-a can be executed will determine how far the β angle will diverge from the reference by the time OMM-a can execute. Nonlinear Monte Carlo analysis was used to determine the maximum expected rates $R1$. Based on the maximum expected rate $R1$ and the safety requirements, it was determined that a 6.5 day OMM lever arm time is necessary.

The two maneuver strategy outlined above can meet safety requirements for avoiding shadow. The other requirement is that the strategy can target a sufficiently stable orbit at the end of OMM-b so that subsequent OMM cycles can continue to control the orbit. This stability requirement can be easily met if OMM-b retargets a 6 state on the original LAMO reference that is already designed to be very stable. It turns out that this is only possible if the initial delivery to LAMO is sufficiently accurate, and the OMM process is begun soon after LAMO begins. It was determined that the first OMM-a should occur within 7 days of the start of LAMO based on Veil (Monte Carlo/optimization) analysis. Also the time between the data cut off for orbit determination and when OMM-a begins to execute is assumed to be three days. The design of both OMM-a and OMM-b must be completed simultaneously. It is possible to update OMM-b after OMM-a executes using the improved knowledge that will be available. However it was found that this is not necessary.

Figure 16 is a timeline of the OMM architecture that was tested to verify the effectiveness of the proposed OMM strategy. The start of LAMO begins at time 0 in Figure 16. The first OMM sequence begins with OMM-a at 7 days (labeled “1”) and OMM-b at 14 days (labeled “2”). The first OMM lever arm is indicated as “Cycle 1” on the timeline. The orbit determination data cut off for the knowledge used to design “Cycle 1” occurs 3 days before OMM-a and is indicated with a red vertical line labeled “DCO 1.” Once the first OMM cycle is complete (red period on the time line), the trajectory is restored (approximately) to the reference trajectory. An adequate maximum duration of each maneuver was found to be 12 hours based on trial and error Monte Carlo runs. The orbit is expected to decay again during the “Coast 1” (green period) on the time line. The duration of the coast period is 6.5 days. At the middle of the “Coast 1” period the design of the second OMM-a/OMM-b sequence is started based on knowledge at “DCO 3”. The second OMM-a/OMM-b sequence is colored dark blue on the timeline. Once the “Cycle 2” OMM-b has executed, the orbit should again be restored (approximately) to the reference trajectory. Two more design and OMM cycles were modeled. No further control is applied after the OMM “Cycle 4” to see what the behavior of uncontrolled orbits is. The momentum wheel desaturation events are modeled as random impulse and are applied at the black vertical tick marks indicated to the right of the label “Desats” on the timeline. Maneuver angle and magnitude error sampling is indicated by diamonds to the right of the labels “Angle sam” and “Mag sam” on the time line in Figure 16.

The result of applying the OMM architecture in Figure 16 to the operating conditions we expect at Vesta is indicated in Figure 17. Figure 17 illustrates the evolution of the β angle during LAMO.

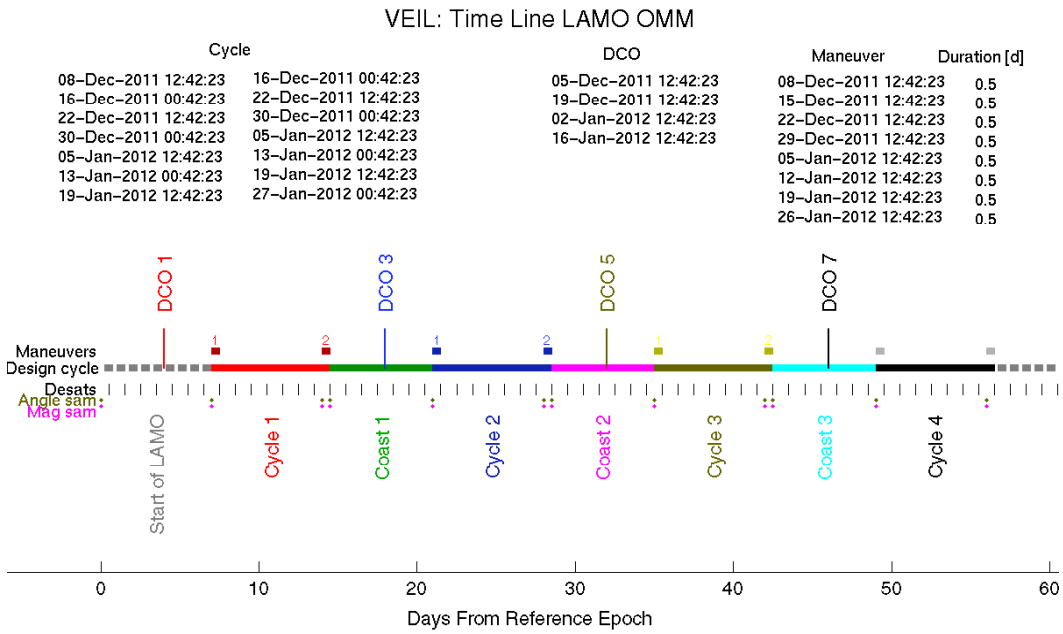

Figure 16. A timeline of the OMM architecture that was tested using Monte Carlo analysis of the sequential design process.

The reference LAMO is indicated as a red line. The slow decrease in LAMO β angle in the reference LAMO would likely disqualify this orbit for real operations. But the ability to control to this reference LAMO still provides a good test of the proposed OMM architecture. A total of 1204 simulations of the OMM architecture under different samplings of knowledge, execution error, and de-saturation impulses are plotted as blue lines in Figure 17. The OMM architecture provided excellent control for all 1204 simulations. When control is terminated (at around day 60 in Figure 17) the β angle departure from the reference is evident. In operations, the OMM process would be continued throughout LAMO.

Figure 18 is the same as 17 except in each of the 1204 simulations the β angle evolution is plotted assuming the failure of OMM-b to execute (green lines). In all 1204 x 4 = 4816 OMM-b failures, all but perhaps 2 stay clear of shadow (around β angle = 39 degrees). This result verifies that the size of OMM lever arm is adequate for spacecraft safety.

CONCLUSION

NASA's Dawn discovery mission will orbit the giant asteroid Vesta beginning in the summer of 2011. Of the four planned near polar science orbits, the lowest planned orbit, Low Altitude Mapping Orbit, is by far the most challenging to design and maintain due to the strong, non-spherical gravity expected there. This paper described the orbit selection process. The true gravity field of Vesta remains highly uncertain. The proposed orbit selection process was shown to work when applied to a fictitious gravity field based on a Hubble space telescope shape model for Vesta assuming uniform density. The outcome of the process described here is a variety of sufficiently stable orbits. Orbital maintenance maneuvers are necessary to counteract the unpredictable impulses resulting from the

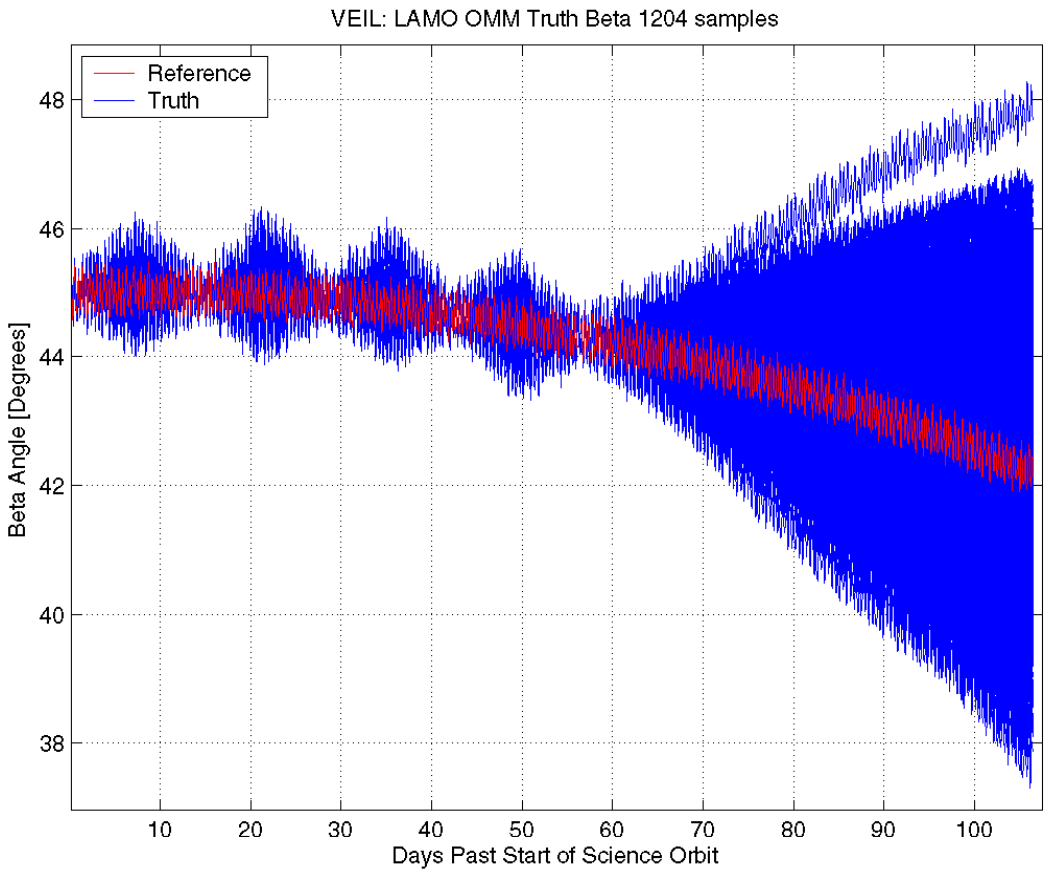

Figure 17. The time evolution of the β angle during LAMO. The reference LAMO is indicated as a red line. 1204 different simulations of the OMM architecture under different samplings of knowledge, execution error, and de-saturation impulses are plotted as blue lines

Dawn spacecraft thruster firings to de-saturate its momentum wheels, uncertainty in Vesta physical properties, maneuver execution error, and the delivery error to the start of LAMO. An architecture for orbital maintenance maneuvers was briefly described and shown to be effective in the operating environment at Vesta.

ACKNOWLEDGMENT

This work was funded by the Dawn Discovery Mission project which is under contract to the National Air and Space Administration.

REFERENCES

[1] M. D. Rayman, T. C. Fraschetti, C. A. Raymond, and C. T. Russell, "Dawn: A mission in the development for exploration of main belt asteroids Vesta and Ceres," *Acta Astronautica*, No. 58, 2006, pp. 605–616.

[2] P. C. Thomas, R. P. Binzel, M. J. Gaffey, A. D. Storrs, E. N. Wells, and B. H. Zellner, "Impact Excavation on Asteroid 4 Vesta: Hubble Space Telescope Results," *Science*, No. 5331 Vol. 277, 1997, pp. 1492–1495.

[3] D. W. Parcher and G. J. Whiffen, "Dawn Statistical Maneuver Design for Vesta Operations," *Proceedings of the AIAA/ASS Astrodynmaics Specialist Conference*, New Orleans, Louisiana, February 13-17, 2011. Paper AAS2011-180.

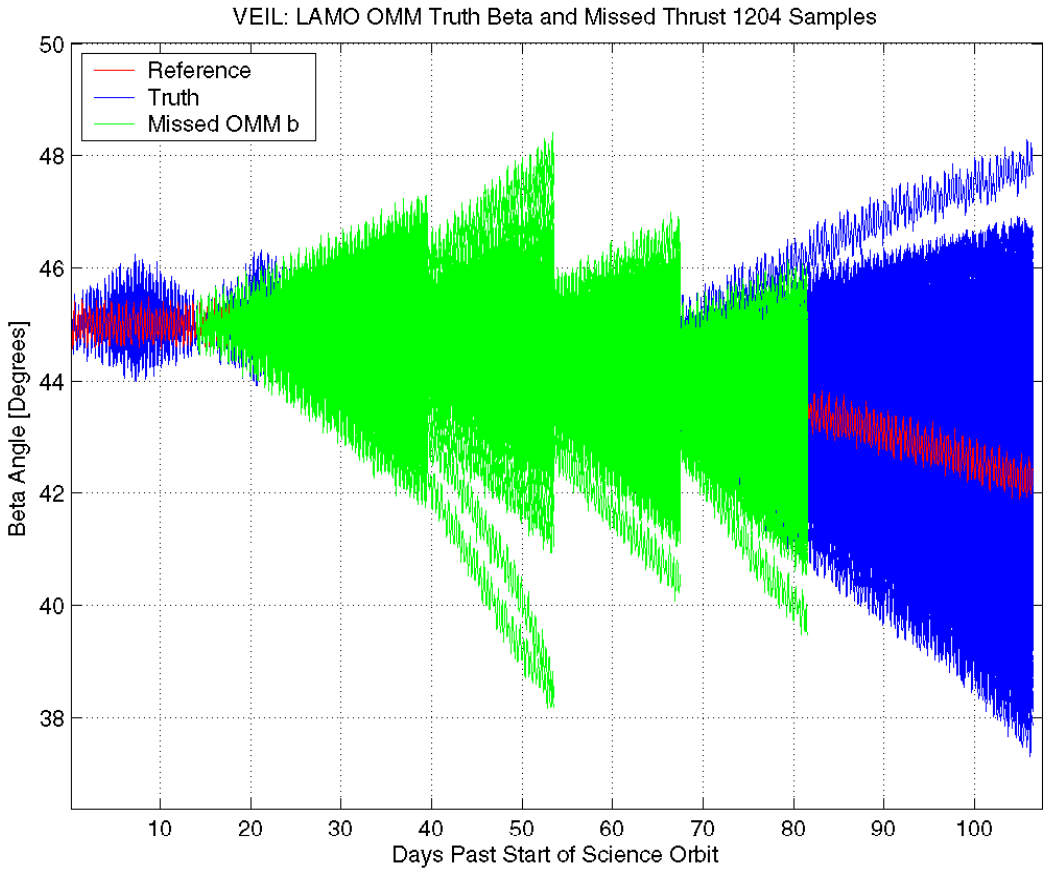

Figure 18. The time evolution of the β angle during LAMO. The reference LAMO is indicated as a red line. 1204 different simulations of the OMM architecture under different samplings of knowledge, execution error, and de-saturation impulses are plotted as blue lines. The β angle evolution when OMM-b fails to execute is plotted in green.

[4] R. v. d. Merwe and E. A. Wan, "Sigma-Point Kalman Filters for Integrated Navigation," *Proceedings of the 60th Annual Meeting of the Institute of Navigation*, Dayton, Ohio, June 7-9 2004.

[5] S. J. Julier and J. K. Uhlmann, "Unscented Filtering and Nonlinear Estimation," *Proceedings of the IEEE*, No. 3 Vol. 93, 2004, pp. 401–422.

[6] G. J. Whiffen, "The Stability of Powered Flight Around Asteroids With Application to Vesta," *Proceedings of the AIAA/ASS Astrodynmaics Specialist Conference*, New Orleans, Louisiana, February 13-17, 2011. Paper AAS2011-186.